



Article

Traces of Local Adaptive Acclimatization Response in the Tracheid Anatomical Traits between Dry and Wet Mesic Norway Spruce (*Picea abies*) Forests in Moravia, Czech Republic?

Dimitrios Tsalagkas ^{1,*} , Tomáš Novák ¹, Marek Fajstavr ^{1,2}, Hanuš Vavrčík ¹ , Vladimír Gryc ¹, Petr Horáček ^{1,2} and Kyriaki Giagli ¹

¹ Department of Wood Science, Faculty of Forestry and Wood Technology, Mendel University in Brno, Zemědělská 3, 613 00 Brno, Czech Republic; tom.novak.olsi@seznam.cz (T.N.); fajstavr.m@czechglobe.cz (M.F.); hanus.vavrcik@mendelu.cz (H.V.); vladimir.gryc@mendelu.cz (V.G.); horacek.p@czechglobe.cz (P.H.); kyriaki.giagli@mendelu.cz (K.G.)

² Department of Xylogenesi and Biomass Allocation, Czechglobe—Global Change Research Institute, The Czech Academy of Sciences, Bělidla 4a, 603 00 Brno, Czech Republic

* Correspondence: dimitrios.tsalagkas@mendelu.cz

Abstract: Norway spruce (*Picea abies*) forests in temperate zones are already reacting to short-term extreme summer heatwaves, threatening the vitality of trees and forest productivity, and can even lead to local and regional dieback events. Examining quantitative wood anatomy can provide helpful information in terms of understanding the physiology mechanisms and related responses of conifer trees to local environmental interactions in relation to tracheid adaptive capacity. This study analysed the tracheid functional anatomical traits (FATs) plasticity of six young Norway spruce trees growing in two mesic research plots with high annual precipitation (~43%) and air temperature differences during 2010–2017. The research plots are located in the sub-mountainous (Rájec Němčice) and mountainous (Bílý Kříž) belts of the Moravia region, Czech Republic. Vapour pressure deficit and cell wall reinforcement index (CWRI) were shown to be the most representative environmental parameters as proxies of dry conditions. Tracheid FATs indicated latewood phenological plasticity sensitivity, with more pronounced variability in the warmer and drier plots. Latewood tracheids of Norway spruce trees grown in the RAJ formed significantly thicker cell walls than BK during the studied period. The observed differences between the two research plots indicate additional support for tracheid cells' hydraulic safety against cavitation and potential traces of adaptive acclimatization response.

Keywords: quantitative wood anatomy; climatic response; cavitation resistance; vapour pressure deficit; cell wall reinforcement index



Citation: Tsalagkas, D.; Novák, T.; Fajstavr, M.; Vavrčík, H.; Gryc, V.; Horáček, P.; Giagli, K. Traces of Local Adaptive Acclimatization Response in the Tracheid Anatomical Traits between Dry and Wet Mesic Norway Spruce (*Picea abies*) Forests in Moravia, Czech Republic? *Forests* **2024**, *15*, 784. <https://doi.org/10.3390/f15050784>

Academic Editors: Mou Leong Tan, Cheng Li, Fei Zhang and Kwok Pan Chun

Received: 3 April 2024

Revised: 25 April 2024

Accepted: 26 April 2024

Published: 29 April 2024



Copyright: © 2024 by the authors. Licensee MDPI, Basel, Switzerland. This article is an open access article distributed under the terms and conditions of the Creative Commons Attribution (CC BY) license (<https://creativecommons.org/licenses/by/4.0/>).

1. Introduction

Trees' growth and forest ecosystems are closely interlinked with climate forcing and variability at short- and long-term scales [1]. Changes in any environmental factor trigger a cascade of modifications at the physiological and morphoanatomical levels of plants, affecting plant growth (meristem activity and morphological development) and productivity [2]. As the most fundamental attributes of woody plants over the life of a tree are the result of short- to long-term physiological responses, xylem tissues are under intensive selective pressure to respond to abiotic and biotic challenges [3,4] adaptively.

The variability of xylem cell anatomy within a population can be very high, reflecting a genetic richness that leads to the selection of new genotypes of the same species (genetic change adaptation fitting into the new environment) and/or phenotypic abilities in terms of acclimatization (potentially reversible physiological responses to environmental variables), which is fundamental for adaptive processes [5]. Phenotypic plasticity is genetically controlled and allows plastic reactions of the functional anatomical traits (FATs),

which permit tree species to withstand a broad range of environmental conditions in which trees live [6]. Phenotypic plasticity is essential in trees' hydraulic strategies concerning water availability, suggesting that tracheid FATs may have allowed conifers to radiate into different habitats [7].

Quantitative wood anatomy, i.e., intra-annual resolved xylem cell anatomical traits along tree ring series, is a methodological approach that operates at the cellular level [8]. This method provides new possibilities in terms of providing better insights into the mechanisms related to year-to-year xylem FATs and the related consequences of environmental interactions on conifers' tree physiology and growth at highly resolved temporal and spatial scales [9,10]. This is achieved by quantitatively investigating the variability of the tracheid FATs within specific tree-ring zones and can provide useful information concerning tracheid cell anatomy and environment [11,12]. Several studies have emphasized a close interconnection between conifer tracheid FATs and seasonal environmental and weather fluctuations, reflecting changes in regional conditions related to these short, sub-annual intervals [8,13–19]. Climate change is expected to intensify regional-scale droughts; therefore, quantifying the extent of plasticity driven by the FATs of the xylem is critical for predicting the tolerance ranges of different species and their resilience to dry conditions [20].

Norway spruce (*Picea abies* (L.) Karst) a late-successional species with slow, early growth and late mean annual increment culmination; is considered to grow better in mesic sites and intermediate-to-high-fertility soils [21]. In addition, Norway spruce, as an intermediately shade-tolerant species, is sensitive to weather conditions, for instance, summer water deficits and soil water recharge in the preceding autumn and early spring [22]. It is also predicted to suffer from warmer and wetter winters [23]. Since 2000, parts of Central Europe have experienced persistent hot and dry periods in summer and non-summer periods [24], leading to a greater risk of precipitation deficits combined with increased temperatures and evapotranspiration [25]. Precipitation deficits can lead to a tight hydrological balance and, potentially, plant water stress [26]; thus, concerns have been raised concerning the ecological stability and adaptation of drought-sensitive Norway spruce trees [22,27,28]. Boden et al. [29] indicated a loss of growth resilience and stress response to decreasing water availability and a relatively limited short-term adaptive capacity to changing climate conditions in tree-ring width (TRW) series of Norway spruce trees located in southwestern Germany in sub-mountainous and mountainous belts.

However, information relating to tree species' adaptive capacity and regional growth resilience to climate change in European forests is complex. Moreover, individual site characteristics may buffer or boost the impacts of heat, drought, and storm events [30]. Focused research is required because trees adapt to local water availability [25] at various temporal and spatial scales [31]. Considering the current environmental changes and their impact on tracheid cells, a better understanding of the environmental effects on dry- and wet-mesic Norway spruce forests with significant precipitation differences and how the anatomy of Norway spruce tracheid cells cope with the harsher climate conditions is decisive.

Cavitation resistance is associated with the 'thickness to span ratio', i.e., the ratio between the double cell wall thickness (CWT) and the conduit lumen radial diameter width (LRD) of tracheid cells. Higher resistance to cavitation requires stronger tracheids with a higher 'thickness to span ratio' to withstand mechanical stress and lower negative pressures [7,32–34]. Therefore, we hypothesized that the Norway spruce trees growing in warmer and drier environments would display greater hydraulic safety, i.e., thicker cell walls and narrower conduits, than in colder and wetter environments due to the increased unfavourable conditions in response to water stress and drought intensity. We also hypothesized that the FATs of the Norway spruce trees in the selected research plots were different concerning local environmental conditions and precipitation regimes, suggesting an adaptive acclimatization response [35–37]. The objectives of this study were (i) to assess the phenotypic plasticity adjustments of tracheid FATs on young Norway spruce trees to environmental variation and (ii) to analyse the correlations between the examined envi-

ronmental parameters (EPs) and tracheid FATs to assess which parameters determine the observed plasticity of tracheid cellular anatomy.

2. Materials and Methods

2.1. Study Sites and Characteristics

Two Norway spruce research plots, located on two experimental ecosystem stations (Figure A1) in the Czech Republic (CZ), part of the Czech long-term ecosystem research network (<https://lter.cz/en/homepage>, accessed on 2 April 2024), the Czech Carbon Observation System (CzeCOS) network (<http://www.czecos.cz/en.html>, accessed on 2 April 2024) and the Integrated Carbon Observation System (ICOS) International Network (<https://www.icos-cp.eu>, accessed on 2 April 2024) [38,39] were studied to account for local variability. Rájec Němčice (RAJ) is situated at a lower altitude (600–660 m a.s.l.) on a hilly slope with NEE exposure in the South Moravian region, while Bílý Kříž (BK) is situated at a higher altitude (800–900 m a.s.l.) on an SSW-oriented planar slope with a mountain ridge terrain [40]. The ecosystem type can be classified as coniferous evergreen forests, and both forest research plots are dominated by a monoculture of Norway spruce trees [41]. Cambisol (RAJ) and podzol (BK) soils crosslinked with several bedrock types and altitudinal zones represent the two major forest soil and associated soil groups, covering over 80% of the CZ territory [42].

From a climatic point of view (Table 1), the RAJ sub-mountainous region is relatively warm and moderately dry, with frequent high-temperature episodes and dry periods, particularly in the summer months [43]. BK experiences a cold and humid environment with high annual precipitation [39,40] and represents the mountainous region conditions of Central Europe [44]. Therefore, this study will assess RAJ as a dry-mesic Norway spruce forest research plot and BK as a wet-mesic Norway spruce forest research plot.

Table 1. Long-term weather data (annual mean air temperature and sum of precipitation) for the 1990–2022 period, according to the records of two nearby stations belonging to the Czech Hydrometeorological Institute (www.chmi.cz, accessed on 2 April 2024).

Long-Term Weather Data	Rájec Němčice (RAJ)	Bílý Kříž (BK)
Mean annual air temperature, °C	7.3 ± 0.8 ¹	7.0 ± 0.7 ²
Mean annual sum precipitation, mm	638.5 ± 93.1	945.1 ± 126.5
Mean air temperature Apr–Sept, °C	13.7 ± 0.9	13.1 ± 0.7
Mean sum precipitation Apr–Sept, mm	409.3 ± 86.4	575.1 ± 131.5

¹ Protivanov meteorological station (ID: B1PROT01; ~675 m a.s.l.; 49°29' N, 16°50' E); ² Bílá Konečná meteorological station (ID: O1BILA01; ~720 m a.s.l.; 49°27' N, 18°31' E).

2.2. Sample Collection and Preparation

Six healthy, young Norway spruce trees were harvested at the donor research plots during the spring of 2018 before the budburst period. All of the selected trees were uniform, with a conical crown, and without visible damage or abnormality on either the stem or the crown. The trees were comparable in size and age. The mean tree height, breast height diameter, and age of Norway spruce trees harvested in the RAJ were 20 m, 18 cm, and 39 years, respectively. Similarly, the mean tree height, breast height diameter and age of Norway spruce trees in the BK were 18 m, 17 cm, and 33 years, respectively. Wood samples of each tree were collected on-site by cutting stem discs (3–4 cm thickness) at breast height immediately after felling. Subsequently, with a small saw, 1 cm wide strips (with a direction from the bark to the pith) of wood were cut from the stem discs. Transversion sections of wood strips were prepared by using a WSL core-microtome [45] and coated with cornstarch-water-glycerol solution (10 g of cornstarch, 8 mL of distilled water, and 7 g of glycerol) to stabilize and prevent the cells from being distorted or broken, as suggested by Schneider and Gärtner [46]. The prepared microsections were stained using Safranin (Waldeck GmbH & Co., Münster, Germany) and permanently mounted on the microscope slides with Euparal (Waldeck GmbH & Co., Münster, Germany).

2.3. Measurements and Statistical Analysis

2.3.1. Tree-Ring Width and Tracheid Anatomical Measurements

The TRW and FATs measurements were conducted cell-by-cell along three radial files within each ring, per year and tree, in each research plot, avoiding areas with visible defects (e.g., reaction wood, traumatic areas). The TRW tracheid FATs used in the study were direct measurements derived from the image analysis program WinCELL Pro 2010 (Regent Instruments, Canada). The analysis was restricted to the tree rings formed in 2010–2017 at the stems' northern alignment to avoid juvenile wood in the young Norway spruce trees [47]. For analysing the xylem structure at the sub-annual time scale, each tree ring was divided into earlywood (EW) and latewood (LW) tree-ring zones, according to Mork's index, which is the ratio between the double CWT and the LRD [48]. The tracheid measurements were assembled into three functional groups related to tree-ring growth, cell growth, and hydraulic safety (Table 2). Within the tree ring, TRW, earlywood width (EWW), latewood width (LWW), and latewood width percentage (LWW%) were calculated. Within each cell, we measured the following FATs: (1) CWT, (2) LRD, (3) the tracheid radial diameter width (TRD), (4) the cell lumen area (CLA), and (5) the cell wall reinforcement index (CWRI). The CWRI is defined as the 'thickness to span' ratio ($[t/b]^2$) [15,33], where t is the double CWT and b is the LRD as the side of a hypothetical square conduit of CLA [49]. During xylem formation and plant secondary growth, inter- and intra-annual changes in the anatomical structure of cells (such as the size of tracheid lumens and walls) in response to EPs also represent the trees' hydraulic architecture, which balances the optimisation of water transport (hydraulic efficiency) against the risk of hydraulic failure (or hydraulic safety) [37]. Xylem hydraulic safety estimated by the CWRI is considered a good proxy for xylem resistance to embolism and cell wall implosion since this ratio is believed to be a surrogate of the tracheid FATs linked to the mechanical and hydraulic properties of trees [19,37,50].

Table 2. A descriptive summary of Norway spruce (*Picea abies*) tree variables used in this study, divided by the functional groups.

Functional Groups	Parameters	Acronym	Unit
Ring growth	Tree-ring width	TRW	mm
	Earlywood width	EWW	mm
	Latewood width	LWW	mm
	Percentage of latewood width	LWW%	%
Cell growth	Cell wall thickness	CWT	μm
	Lumen radial diameter	LRD	μm
	Tracheid radial diameter	TRD	μm
	Cell lumen area	CLA	μm^2
Hydraulic safety	Conduit cell wall reinforcement index	CWRI	-

To calculate the TRD based on the relative position (RP) of each tracheid cell within a tree ring, we used the following equations [51]:

$$TRD = \frac{1}{2}(2CWT) + LRD + \frac{1}{2}(2CWT) \quad (1)$$

and

$$RP = \frac{X_n}{N} \quad (2)$$

where $2CWT$ is the thickness of a double cell wall, X_n is the rank of a cell in the tree ring increment, and N is the total number of cells. The LWW% was calculated as the ratio of LWW to TRW [52]:

$$LWW\% = \frac{LWW}{TRW} \times 100 \quad (3)$$

Since the number of tracheids varied among radial files among trees and within tree rings of each tree ring, tracheid FATs were standardized and then averaged based on the relative position of each tracheid within the ring [53].

2.3.2. Meteorological Parameters and Vapour Pressure Deficit

A multi-year dataset of half-hourly eddy covariance measurements made by the CzeCOS network instruments per research plot, recorded above the canopy, was used for this study. The air temperature (T_{air}) and relative humidity (RH) profile records were taken with EMS33 temperature and humidity sensors (EMS Brno, CZ). In contrast, the amount of precipitation (PRCP) was recorded using 386C Met One precipitation gauge instruments (Met One Instruments, USA). The daily-resolved values for mean T_{air} , RH and the sum of PRCP for the studied period of 2010–2017 were calculated. The mean annual T_{air} at the RAJ during 2010–2017 was 7.8 ± 0.7 °C, i.e., 1.2 °C greater than the BK (mean annual T_{air} was 6.6 °C). Accordingly, the mean annual sum PRPC at the RAJ was 660 ± 94 mm, i.e., 42.81% less than the mean annual sum PRPC at the BK (1154 ± 178 mm) (Figure 1).

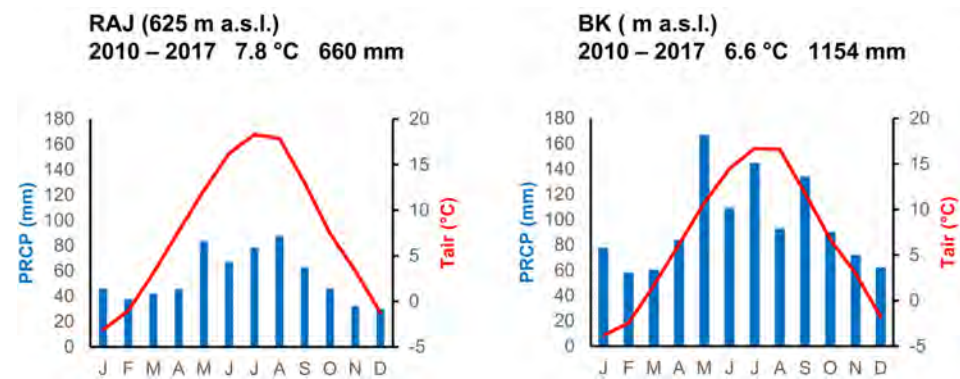


Figure 1. Mean monthly weather data of the studied research plots during 2010–2017 (T_{air} , air temperature; PRCP, sum of precipitation).

The vapour pressure deficit (VPD) reflects the effect of T_{air} and PRCP on the RH and transpiration demand. It is often monitored as a proxy for plant water stress, stimulating stomatal closure and photosynthetic carbon fixation [54]. Above-ground atmospheric demand for moisture was represented by the VPD (kPa), according to the equation:

$$VPD = \left(1 - \frac{RH}{100}\right) \times SVP \quad (4)$$

where SVP is the saturated vapour pressure for a given temperature. SVP was estimated according to Tetens equation:

$$SVP = 0.61078 \exp\left(\frac{17.27T_{air}}{T_{air} + 237.3}\right) \quad (5)$$

where T_{air} is in °C and SVP in kPa [55]. A VPD value of 1.5 kPa (VPD1.5) was chosen as an ‘extreme’ threshold, above which stomata close, representing the extremely dry air [56].

2.3.3. Standardized Precipitation Evapotranspiration Index (SPEI)

Variations in drought severity, duration, and timing complicate the situation, and it is challenging to quantify the tree species’ physiological and anatomical adjustments to cope with drought [22]. Frequency, duration, and severity are the most critical characteristics of drought, and they depend on the established time scales as a function of the period. As time scales become larger, each new month has less impact, and drought becomes less frequent and of longer duration [57]. A one-month SPEI (SPEI-1) resolution was chosen to cover short drought episodes since these affect drought-sensitive tree species on shallow

soils, as Fonti and Babushkina [17] suggested. Short-term interactions are preferable in assessing meteorological drought to soil moisture drought because they capture drought onsets and short-term severe bouts of drying that are potentially blunt in more prolonged interactions [58].

The impact of meteorological droughts is a complex, multisectoral, spatially variant and context-dependent phenomenon with different responses as a function of hydrology subsystems, vegetation, water resources management and seasonal time scales, making it difficult to quantify its characteristics and may lead to over- or underestimating reliable thresholds [59,60]. Thus, it is more appropriate to use an objective, location-specific method when defining drought thresholds to properly quantify drought seasonality, severity, and duration [59]. We adopted the drought definition of [57] as proposed by Parente et al. [61] and Spinoni et al. [62] to identify the drought events (DEs), which started once the analyzed SPEI-1 indicator drops below the corresponding value to a given negative standard deviation ($\text{SPEI-1} \leq -1.0$) for at least two consecutive months and finished when this indicator rises above zero ($\text{SPEI-1} \geq 0$). If, during the DE, at least two successive months show extreme drought conditions, the event would be considered extreme. Drought frequency displays the number of events, while drought duration demonstrates the number of months that a DE lasts. The assessment of meteorological DE intensity was classified into four classes, according to the increasing negative SPEI-1 values of less or equal to -1.0 [61]: (i) mild ($-1.0 < \text{SPEI-1} \leq 0$), (ii) moderate ($-1.5 < \text{SPEI-1} \leq -1.0$), (iii) severe ($-2.0 < \text{SPEI-1} \leq -1.5$), and (iv) extreme ($\text{SPEI-1} \leq -2.0$).

2.3.4. Statistical Analysis

Based on the monthly Tair and PRCP data, we quantified the meteorological drought according to the SPEI climatic water balance drought index using the Thornthwaite R v. 4.1.1. package SPEI [63]. Daily records of mean Tair, RH, PRCP, and VPD values for the period 2010–2017 obtained from the meteorological stations located at the research plots were used to test the relationships between the FATs (i.e., CWT, TRD, CLA, and CWRI) and the EPs. The tested EPs (Tair, RH, PRCP, and VPD) were arranged in fixed intervals of 15-day time windows from the beginning of April till the end of July in the year of tree-ring formation and from the beginning of July till the end of October for the EW and LW tree-ring zones, respectively. The relationships between the EPs between the research plots and medial values of Norway spruce tracheid FATs in each tree-ring zone were computed using the non-parametric Kendall's tau rank correlation coefficient, which accounts for a smaller sample size [64]. Short time intervals of 15-day long time scales were chosen to capture better the dependency of the tracheid of FATs on short-time responses [9]. Correlations between the EPs and FATs were considered significant if the p -value was <0.05 .

Finally, we adopted the non-parametric Mann–Whitney test to compare EPs between the two research plots, which is more robust to possible outliers and distribution skewness [65]. Similarly, to compare dry-mesic (RAJ) vs. wet-mesic (BK) FATs on the tracheids of Norway spruce trees without considering the time dimension, we used the non-parametric Mann–Whitney test, a method used to contrast two groups without considering any distribution information on the population [54]. All non-parametric tests were performed using the Statistica 13.4.0.14 analysis package (TIBCO Software Inc., Palo Alto, USA).

3. Results

3.1. Environmental Parameters

The trend agreement among the examined EPs between the two research plots (Figure 2) showed that the variations in time series resolutions of 15-day intervals follow a similar pattern across the investigated period of 2010–2017. Apart from the existing PRCP differences, we can also detect the low RH and high VPD values that occurred at both research plots during the summer months (July–August) of 2015 and, to a lesser extent, in 2013.

The interannual variability of the meteorological parameters (Tair and PRCP) during 2010–2017 portrayed a warmer and drier research plot in RAJ compared to the wetter and

slightly colder conditions in the BK (Table A1). The number of VPD1.5 days, i.e., the days in which the extreme threshold value of VPD1.5 occurred, as was expected mainly occurred during the summer months of July and August. Interestingly, the years (2012 and 2014 during the spring period and 2013 and 2015 during the summer period) and the number of days with the increased VPD1.5 were almost identical for both research plots. However, during the most severe year of 2015, the number of VPD1.5 days in the driest RAJ was double when compared to the wettest BK, i.e., 18, and 9 days, respectively.

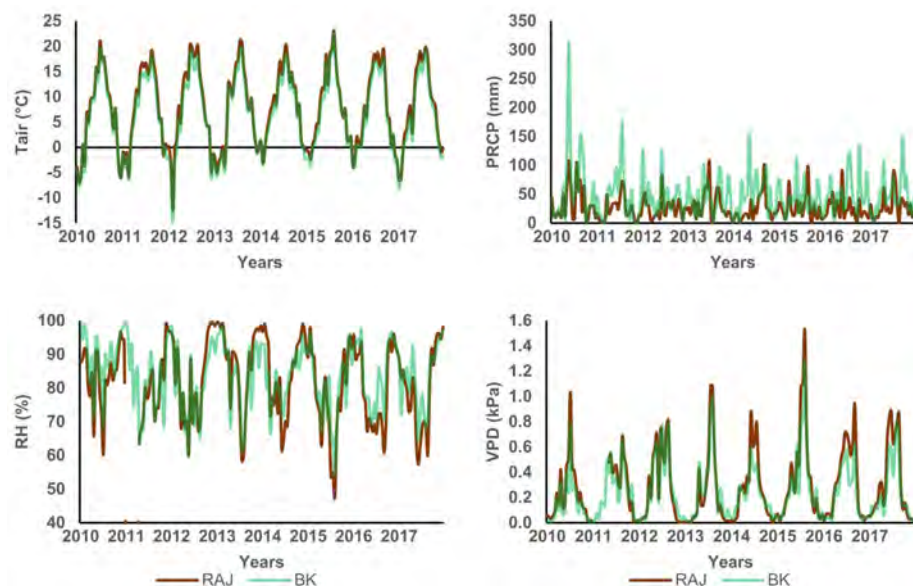


Figure 2. Time series of the mean values of the environmental parameters (EPs) for the 2010–2017 period for the Rájec Němčice (RAJ) and the Bílý Kříž (BK) plot (Tair, air temperature; PRCP, precipitation; RH, relative humidity; VPD, vapour pressure deficit).

Seasonal Mann–Whitney U test analyses during the growing season (April–September), as well as between the spring (April–June) and summer (July–September) sub-annual intervals, were performed to assess statistical differences in the EPs between the two studied research plots (Table 3, Figure A2). Tair, PRCP, and VPD were determined to be statistically significantly different during the growing season. Accordingly, only Tair and PRCP of the sub-annual periods were statistically significant, while RH and VPD were not. Yet, we should not overlook the higher calculated mean VPD value in the RAJ (0.56 ± 0.15 kPa) when compared to BK (0.45 ± 0.13 kPa). Since the variability of EPs during the 2010–2017 period was indicated between the two research plots, we expect that any differences in the phenotypic plasticity of the tracheid FATs of Norway spruce trees in the research plots would reflect the adjustment of the anatomy of tracheids' to environmental variations.

3.2. Drought Assessment

We compared drought frequency, duration, and intensity during the 2010–2017 reference period to investigate the spatial and temporal distributions between the RAJ and BK plots. During this period, we counted two DEs for RAJ and one DE for the BK plot, respectively (Figure 3). RAJ's first shorter duration DE occurred from January to February 2011 (two months), while a prolonged DE of seven months was detected from December 2013 to June 2014. Similarly, a quite dry period of three months, but not a DE in response to the definition, was also identified for the BK plot from January to March 2014. The only DE that occurred in BK was during the spring of 2012 for two months (April to May 2012). No extreme conditions were detected, and approximately 3% and 15% of the total months were detected as severe and moderate drought months (Table 4).

Table 3. Seasonal environmental parameters (EPs) for the studied research plots during the 2010–2017 period. Mean air temperature, relative humidity, and vapour pressure deficit ($T_{air_{2010-2017}}$, $RH_{2010-2017}$, $VPD_{2010-2017}$), and mean sum precipitation ($PRCP_{2010-2017}$) for each duration of the growing and sub-annual period (April–September, April–June, and July–September) are presented. The \pm symbol depicts the standard deviation values. Asterisks denote significant differences between the two research plots (ns—not significant, * $p < 0.05$, ** $p < 0.01$).

	Annual		April–September			April–June			July–September		
	RAJ	BK	RAJ	BK	<i>p</i> -Value	RAJ	BK	<i>p</i> -Value	RAJ	BK	<i>p</i> -Value
$T_{air_{2010-2017}}$ (°C)	7.8 (±0.7)	6.6 (±0.6)	14.2 (±0.6)	12.7 (±0.4)	**	12.0 (±0.8)	10.5 (±0.6)	**	16.4 (±0.7)	15.0 (±0.7)	**
$RH_{2010-2017}$ (%)	82.3 (±3.2)	83.7 (±3.0)	74.4 (±4.5)	78.1 (±4.1)	ns	75.0 (±5.8)	78.2 (±4.5)	ns	73.8 (±6.0)	78.1 (±5.4)	ns
$PRCP_{2010-2017}$ (mm)	660.3 (±94)	1153.7 (±178.6)	425.8 (±104.5)	732.1 (±239.2)	**	196.9 (±67.7)	360.4 (±132.5)	*	228.8 (±71.5)	371.7 (±113.6)	*
$VPD_{2010-2017}$ (kPa)	0.29 (±0.05)	0.25 (±0.05)	0.49 (±0.09)	0.39 (±0.08)	*	0.41 (±0.10)	0.34 (±0.07)	ns	0.56 (±0.15)	0.45 (±0.13)	ns

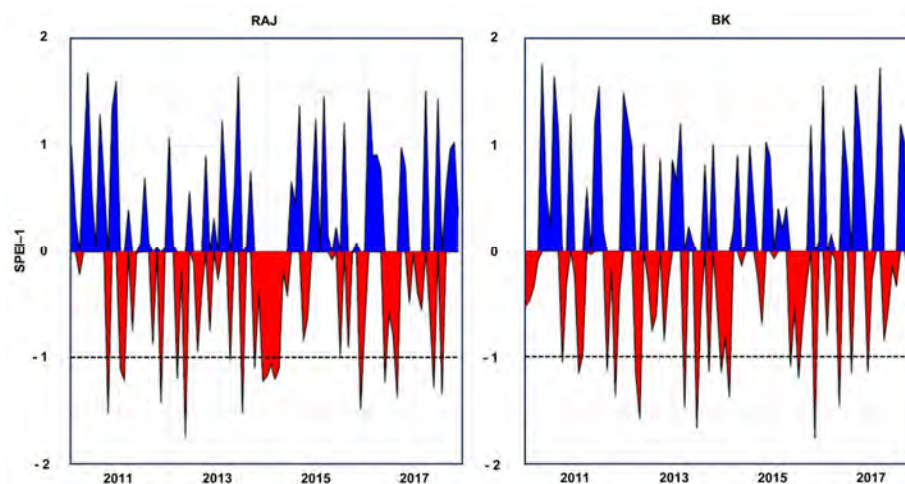


Figure 3. Running 1-month time scale Standardized Precipitation Evapotranspiration Index (SPEI-1) values from January 2010 to December 2017 in the RAJ and BK research plots. Positive values (blue) indicate cooler and wetter conditions, and negative values (red) indicate warmer and drier conditions. SPEI-1 was calculated with a Thornthwaite-type water balance. Dashed lines indicate the -1.0 threshold as the benchmark of drought stress conditions (moderate, severe, and extreme).

Table 4. General drought conditions (GDCs) were assessed with SPEI-1 and drought classes (mild, moderate, severe, and extreme) for the reference period of 2010–2017. Relative values are equal to the ratio between the number of drought months and the total number of months.

Plots	GDCs	Drought Class			
		Mild	Moderate	Severe	Extreme
RAJ	46.8%	27 (28%)	16 (17%)	2 (2%)	0 (0%)
BK	53.1%	34 (35%)	14 (15%)	3 (3%)	0 (0%)

3.3. Tree-Ring Growth Variability

Norway spruce trees grown in the dry-mesic (RAJ) and wet-mesic (BK) plots did not differ in diameter, height and age. In general, drier conditions of the RAJ plot during the 2010–2017 growing seasons promoted wider LWW, apart from the 2015 summer drought of July–August (based on VPD values and the number of VPD1.5 days), in which LWW sharply dropped. Specifically, the mean TRW and LWW% values in the RAJ were 1.9 ± 0.6 mm and $30.0 \pm 7.5\%$, while in the BK 2.13 ± 0.4 mm and $19.5 \pm 4.2\%$. Mann–Whitney *t*-tests demonstrated statistically significant differences in the EWW ($p < 0.05$) and

LWW% ($p < 0.01$). At the same time, TRW and LWW were found not to be significantly different (Table 5).

Table 5. Intra-annual mean values tree-ring width (TRW), earlywood width (EWW), latewood width (LWW), and latewood width percentage (LWW%).

Years	TRW (mm)		EWW (mm)		LWW (mm)		LWW%	
	RAJ	BK	RAJ	BK	RAJ	BK	RAJ	BK
2010	2.27	2.00	1.47	1.64	0.80	0.36	35.2%	18.0%
2011	2.94	2.66	1.96	2.36	0.98	0.3	33.3%	11.2%
2012	2.17	2.47	1.58	1.86	0.59	0.61	27.2%	24.7%
2013	2.02	1.92	1.52	1.55	0.50	0.37	24.7%	19.3%
2014	1.62	2.65	1.10	2.05	0.52	0.60	32.7%	22.6%
2015	1.04	1.60	0.88	1.25	0.16	0.35	15.4%	21.9%
2016	1.88	2.17	1.30	1.80	0.58	0.37	31.4%	17.0%
2017	1.22	1.53	0.72	1.53	0.50	0.40	40.1%	21.1%
2010–2017 (st. dev.)	1.9 (± 0.6)	2.13 (± 0.4)	1.32 (a) (± 0.4)	1.76 (b) (± 0.3)	0.58 (± 0.2)	0.42 (± 0.1)	30.0% (a) ($\pm 7.5\%$)	19.5% (b) ($\pm 4.2\%$)

Letters denote statistically significant differences.

Although detecting long-term trends on such a relatively short time series of an 8-year analysis is challenging, most of the phenotypic plasticity variability was primarily related to changes occurring at the LW tree-ring zone. Based on the standardized tracheidograms and Mork's index, we observed a more considerable year-to-year variability in the LW tree-ring zone, which was more prominent in the drier RAJ. We also estimated that LW formation occurred earlier in the RAJ within the summer months, as illustrated in Figure 4.

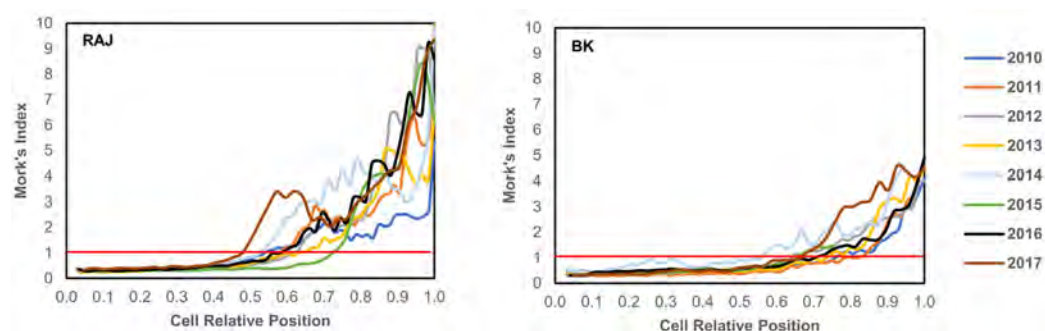


Figure 4. Interannual variability (2010–2017) of earlywood (EW) and latewood (LW) of the standardized tracheid cells within the Norway spruce (*Picea abies*) tree ring. The red line shows the boundary between the EW and LW tracheids as determined by Mork's index and the tracheid cells' relative position.

3.4. Sub-Annual Tracheid Anatomical Variability

The results indicate substantial changes in the sub-annual distributions and median values of tracheid FATs within the tree-ring zones between the two research plots (Table 6). Tracheid size (TRD and CLA) was found to be statistically significantly different in the EW tree-ring zone and CWT only in the LW tree-ring zone. Median CWRI, despite not being statistically significant (presumably due to the substantial variable values), was more than double in the RAJ (2.44 ± 1.9) compared to the CWRI (1.01 ± 0.5) in the BK. The results of this study suggest a downscaling of cell size (i.e., TRD and CLA) and the upscaling of CWT in the tracheid cells relating to Norway spruce tree ring growth in both research plots.

Table 6. Statistics describing the median values of measured and derived functional anatomical traits (FATs) of the Norway spruce trees in the dry-mesic RAJ (Rájec Němčice) and wet-mesic BK (Bílý Kříž) research plots.

FATs	Earlywood (EW)		Latewood (LW)	
	RAJ	BK	RAJ	BK
CWT (μm)	3.3 \pm 0.4	3.3 \pm 0.3	6.9 \pm 0.7 (a)	5.3 \pm 0.3 (b)
TRD (μm)	41.1 \pm 3.1 (a)	35.9 \pm 1.7 (b)	25.2 \pm 3.9	22.5 \pm 2.0
CLA (μm^2)	920.9 \pm 131.8 (a)	746.7 \pm 94.2 (b)	150.1 \pm 57.0	200.9 \pm 54.9
CWRI	0.04 \pm 0.01	0.05 \pm 0.02	2.44 \pm 1.9	1.01 \pm 0.5

Values are presented separately for EW and LW. Data are medians \pm SD and correspond to the 2010–2017 reference period. Different letters indicate significant ($p < 0.05$) differences based on Mann–Whitney tests. Abbreviations of variables are CWT, cell wall thickness; TRD, Tracheid radial diameter; CLA, cell lumen area; CWRI, cell wall reinforcement index.

Figure 5 depicts the interannual variation in the FATs of the Norway spruce trees grown in the relatively warm and moderately dry RAJ area that has more frequent summer heatwaves compared to BK, with its cooler and higher annual precipitation. We observed that LW CWT and/or LW LRD in the Norway spruce trees located at the RAJ was reduced when unfavourable environmental conditions occurred, such as during short-term summer heatwaves with several days of high evapotranspiration demand (the year 2015, 18 days VPD1.5 threshold value) or after a prolonged DE during the 2014 winter-spring season.

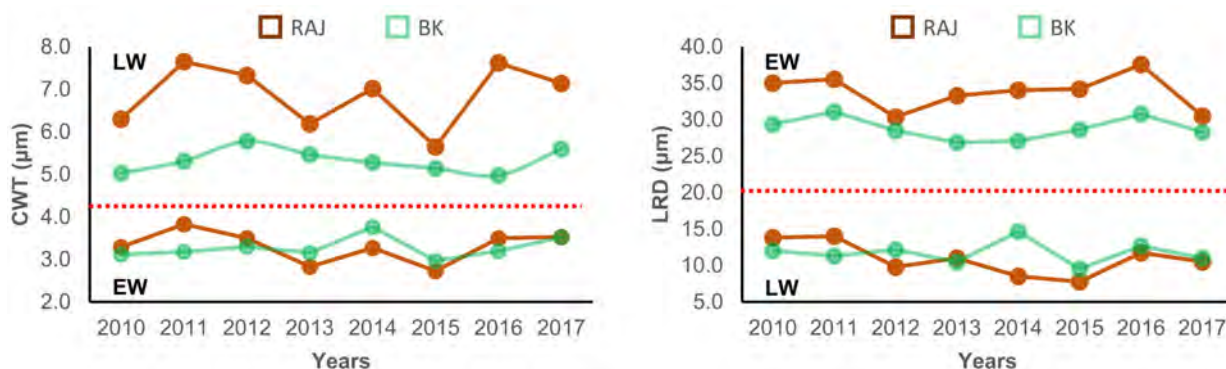


Figure 5. Interannual changes in median CWT and LRD were grouped per tree-ring zone (EW, earlywood; LW, latewood) and research plot (RAJ, Rájec Němčice; BK, Bílý Kříž) from 2010–2017. Horizontal red dotted lines indicate the boundary within each tree-ring zone.

3.5. Environment Parameters–Tracheid Functional Anatomical Traits Relationships

Within this study, we considered the April–June period more relevant to the EW tree-ring zone and the July–September period for the LW tree-ring zone, respectively. Furthermore, based on the lag in the EW–LW transition of the Norway spruce tracheids between the two plots, as can be observed in Figure 4 (according to Mork’s index and cells’ relative position), we considered July as the EW–LW transition month, yet also representing partly the LW tree-ring zone in the RAJ plot and the EW tree-ring zone in the BK plot. We also considered October since it is usually a month in which LW tracheids of Norway spruce trees are still forming.

The FATs in response to the EPs in the Norway spruce trees growing in the two plots showed seasonal and sub-annual variations, with VPD and PRCP being the most important EPs during tracheid formation. The contrasting positive or negative correlations illustrate the impact of EPs in each tree-ring zone by enlarging or narrowing CWT and TRD size, especially during the hottest summer months of July and August. Mainly, EPs were more influential in the warmer and drier RAJ rather than the colder and wetter BK (Figures 6 and 7).

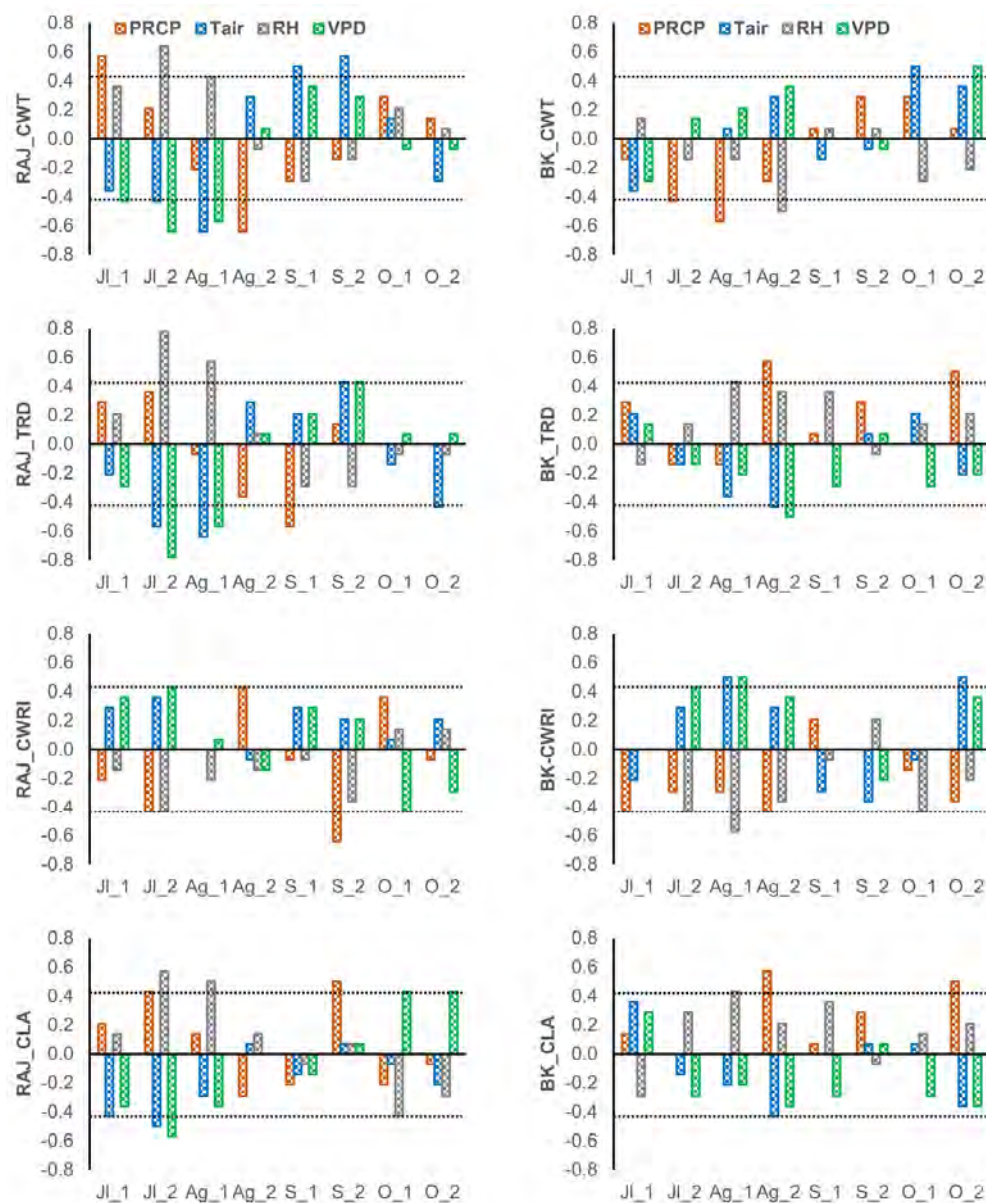


Figure 6. Kendall tau correlation coefficients between the studied EPs (PRCP, Tair, RH, and VPD) and the median values of the tracheid FATs (CWT, TRD, CLA, and CWRI) in the EW tree-ring zone of the Norway spruce trees in the RAJ and BK plots for the period 2010–2017. Months are abbreviated by letters (Ap, April; M, May; Jn, June; Jl, July). Numbers 1 and 2 denote the first half (1–15 days) and second half (16–30 days) time intervals of each month, respectively. Horizontal dotted lines indicate a threshold for significant correlation at $p < 0.05$.

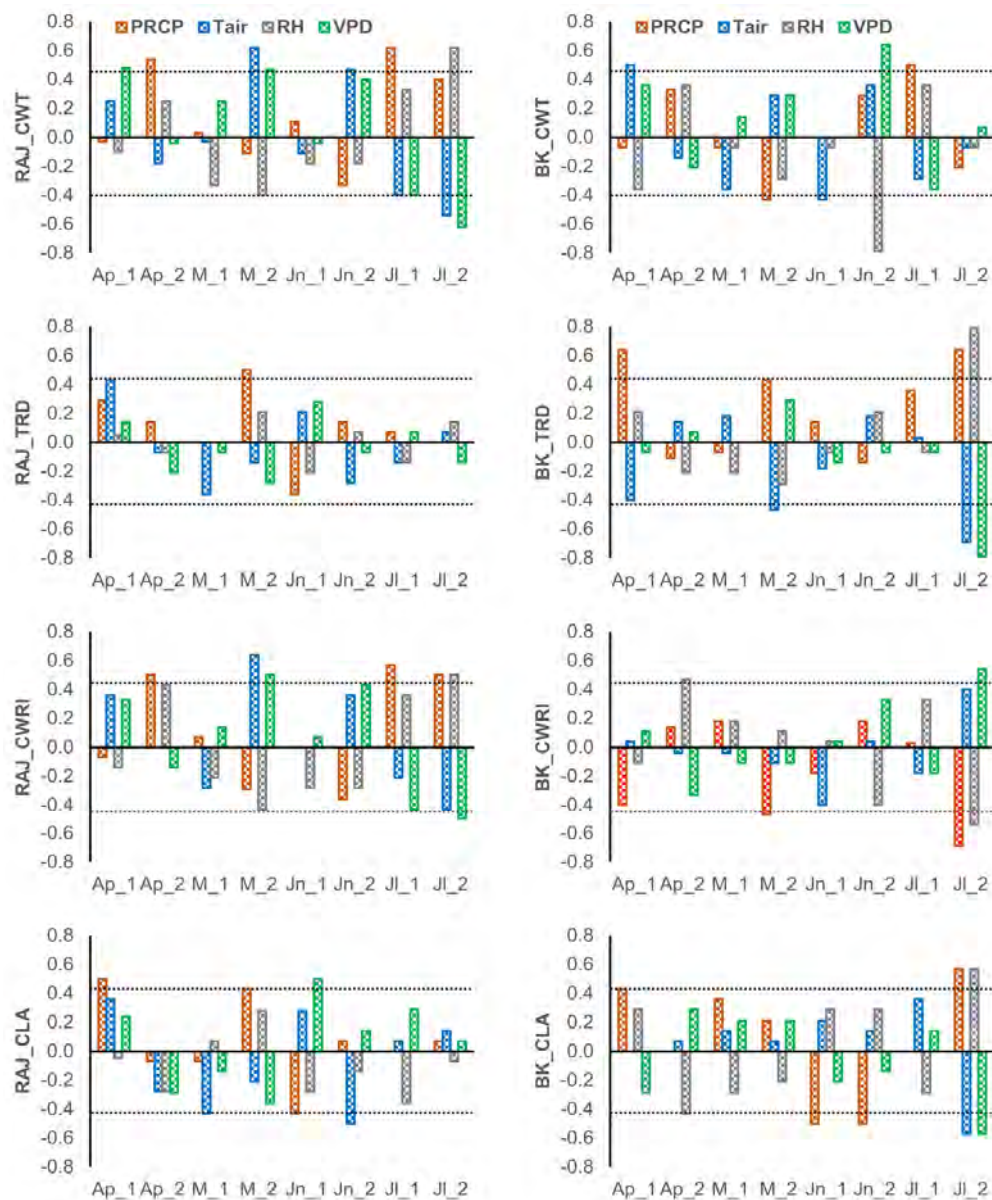


Figure 7. Kendall tau correlation coefficients between the studied EPs (PRCP, Tair, RH, and VPD) and the median values of the tracheid FATs (CWT, TRD, CLA, and CWRI) in the LW tree-ring zone of the Norway spruce trees in the RAJ and BK plots for the period 2010–2017. Months are abbreviated by letters (Ap, April; M, May; Jn, June; Jl, July). Numbers 1 and 2 denote the first half (1–15 days) and second half (16–30 days) time intervals of each month, respectively. Horizontal dotted lines indicate a threshold for significant correlation at $p < 0.05$.

4. Discussion

4.1. Tree-Ring Growth Traits

The amount of EWW and LWW has been demonstrated to play a prominent role in regulating xylem hydraulic safety and efficiency, wood density, and the mechanical functioning of cells. The climate also strongly affects LWW% [19]. In our study, LWW% in the drier RAJ was approximately 42% higher than in the wetter BK and was statistically significant. In addition, the EWW of RAJ was significantly shorter than the EWW measured in BK. Luostarinen et al. [66] report that a higher growth rate is believed to increase the EWW, while the amount of LWW remains relatively constant in Norway spruce. Further, a wider EWW indicates more effective tree water use [67].

4.2. Tracheid Anatomy Traits and Latewood Plasticity Sensitivity

Short-term heatwaves during the summer months of July–August or long-term drought events had a perceptible effect on LW plasticity and sensitivity in the warmer and drier RAJ. The diverse and statistically significant differences in the tracheid FATs of the Norway spruce trees between the two research plots of RAJ and BK demonstrate the phenotypic plasticity and adaptability to the local environmental conditions. EW tracheids of the Norway spruce trees in the dry-mesic RAJ formed larger CLA and almost identical CWT compared to the Norway spruce trees in the wet-mesic BK, while LW tracheids presented narrower sizes and thicker cell walls. Our findings on Norway spruce trees seem to support the conclusions reported by Björklund et al. [14], Piermattei et al. [19], and Rathgeber [68] that conifers may enhance the following: (i) conduction efficiency during the spring period by influencing EW TRD, (ii) water conduction security during the summer period by influencing LW CWT, and (iii) LW is probably the tree-ring zone involved in adaptive responses to climate and environmental changes.

Despite presenting higher year-to-year variability, the CWT of the LW tracheid cells in the dry RAJ was always thicker than that of the LW tracheid cells in the wet BK during the 2010–2017 period. An experimental drought treatment in Norway spruce trees demonstrated changes in xylem cell anatomy traits, with drought-treated trees presenting new cells with a high proportion of thick cell walls and narrower lumen diameters after the experiment's onset. On the contrary, irrigated trees had generally thinner cell walls and wider lumen diameters [34]. Thicker cell walls in conifer species, including Norway spruce grown in drier environments, have also been suggested in other studies as being a reinforcement strategy relating to cavitation resistance to water stress [33,49,67]. Thick cell walls reduce the water flow due to a reduced CLD and increase the water flow path through pits, consequently increasing cavitation resistance [7].

Higher cavitation resistance is associated with lower negative sap pressure, requiring tracheids with a higher CWRI to resist mechanical stress [4]. Pittermann et al. [69] concluded that variation in the CWRI was determined by narrowing lumen diameter rather than thickening cell walls. In contrast, Bouche et al. [32] and Rosner et al. [70] demonstrated that CWT—which is genetically largely determined—and not the LRD, is the critical factor in the collapse of tracheid walls. This study further confirms the usefulness of this index as an indicator of the dry conditions that occurred on the research plots. We believe that the LW differences observed at CWRI values between the two research plots, as well as the interannual observations during the summer months of 2015 or after a prolonged dry winter-spring period is a combined result of the interaction performed in both these anatomical traits (i.e., CWT and LRD). Reductions in both tracheid size and CWT and increased hydraulic safety were explained as being plastic responses to the drought experienced by Norway spruce trees in a mountainous, dry environment in the alpine Swiss region [15].

Although a reduction in the tracheid cell lumina of LW tracheids is beneficial to increasing hydraulic safety, signs of reduced LWW% (~16%) and thin-walled tracheids (5.65 μm) of the Norway spruce trees at RAJ during 2015 compared to the other years, according to Liang et al. [71], can be a mark of water stress in conifer trees. The FATs results of our study also confirmed this conclusion. The summer drought of 2015 was documented in CZ during a record year with high annual fluctuations of anomalous warm days [65] and seasonal dry atmospheric circulation during the April–September vegetation period [72], which was also the case in the Central Europe region [73,74].

4.3. Tracheid Anatomy Traits and Environmental Parameters

Trnka et al. [75] identified that the trends in actual evapotranspiration from July to September are highly dependent on PRCP but are also sensitive to reference evapotranspiration driven by the evaporative demand of the atmosphere. In our study, these EPs were statistically significant during the spring (April–June) and summer (July–September) sub-annual periods between the RAJ and BK plots. In addition, Mensah et al. [76] ob-

served reduced forest productivity at both research plots and the sensitivity of both spruce forest plots to the VPD and Tair, especially at the drier RAJ. These outcomes agree with our findings since (i) VPD was found to be highly correlated with the FATs of Norway spruce tracheids, and (ii) mean VPD was higher in the dry-mesic RAJ compared to the wet-mesic BK; however, there were no statistically significant differences between each sub-annual period.

Despite the fact that, in the context of climate change, meteorological factors such as Tair and PRCP significantly influence evapotranspiration, they are not the only driving factors [77,78]. The effect of evapotranspiration is more complex, as seen in the dry RAJ, since the number of VPD1.5 days during the summer period of 2012 and 2016, two years with low PRCP and high Tair, were 2 and 0 days, respectively. The adequacy of water and the extent of vegetation factors also directly affect the actual evapotranspiration besides the meteorological factors [78]. Moreover, it is generally accepted that evapotranspiration is limited by available soil moisture when the soil moisture content is low, and it responds more to variability in meteorological and atmospheric conditions when there is sufficient soil moisture [77].

Along with its direct impact on plant physiology, high VPD increases water loss rates from moist soils. A drier atmosphere naturally demands more water from the soil surface [2]. Low PRCP is associated with an increased probability of hot days and higher Tair, which can further deplete soil moisture [58]. In this sense, we could consider that summer VPD also partly depicts PRCP and soil water deficits when soil moisture data are unavailable. In this study, we did not consider soil type characteristics. Soil characteristics also significantly affect moisture availability and soil water deficits [22], which could not be captured through the investigated EPs. The relatively high proportion of Norway spruce trees grown in cambisol-type soils (RAJ) instead of podzol-type soils (BK) can be partly associated with their higher clay content and more frequent hydromorphic properties [79].

5. Conclusions

Intra-annual analysis and high phenotypic plasticity on the xylem traits of Norway spruce in the studied research plots potentially point to adaptive acclimatization response mechanisms and a more safety-oriented, water-conducting system influenced by the local environmental conditions. Specifically, the young Norway spruce trees growing in the warmer and drier RAJ presented the following xylem structure differences: (i) on the size of the CWRI by adjusting CWT and LRD dimensions and (ii) by forming tree rings with increased LWW% and higher number of LW tracheids, relevant to the BK. Moreover, the presence of thicker CWT on LW cells to withstand higher rates of negative xylem pressure and, thus, increased cavitation resistance against the harsh summer conditions potentially provides an additional indication of adaptation to the local environmental conditions. Additionally, the interannual analysis revealed that in 2015 and 2013 years, which were characterized by disturbance regimes of heatwaves during the summer months (July–August) and days with high evapotranspiration demand or after prolonged drought events, such as the winter-spring in 2014, were formed LW tracheids with thinner cell walls in the warmer and drier RAJ.

Norway spruce is Europe's most widespread conifer species, with a high economic and ecological value. The practical outcome that the seasonal RH and VPD values were not statistically significant between the two research plots might indicate that the long-term resilience and function of Norway spruce trees growing in wet-mesic forest ecosystems might also be affected if days with high evapotranspiration demand and water deficit will continue to rise. However, understanding species' adaptive capacity and response adaptation to warmer and drier environmental conditions is multidisciplinary and still challenging.

Author Contributions: Conceptualization, H.V., V.G. and P.H.; Methodology, H.V., V.G. and P.H.; Validation, D.T., P.H. and K.G.; Investigation, T.N. and D.T.; Formal analysis, P.H., K.G. and D.T.; Resources, M.F., H.V., V.G. and P.H.; Data curation, D.T.; Writing—Original draft preparation, D.T.; Writing—Review and editing, D.T., V.G., H.V., M.F., K.G. and P.H.; Visualization, D.T. and H.V.; Supervision, V.G., P.H. and K.G.; Project administration D.T. and K.G.; Funding acquisition, K.G. All the authors critically reviewed and approved the final version of the manuscript submission. All authors have read and agreed to the published version of the manuscript.

Funding: This study was supported by funding from the Internal Grant Agency (IGA) of the Faculty of Forestry and Wood Technology at Mendel University in Brno under Grant Agreement No. LDF_VP_2021027. This study is also part of the ASFORCLIC project that has received funding from the European Union’s Horizon 2020 research and innovation programme under Grant Agreement No. 952314.

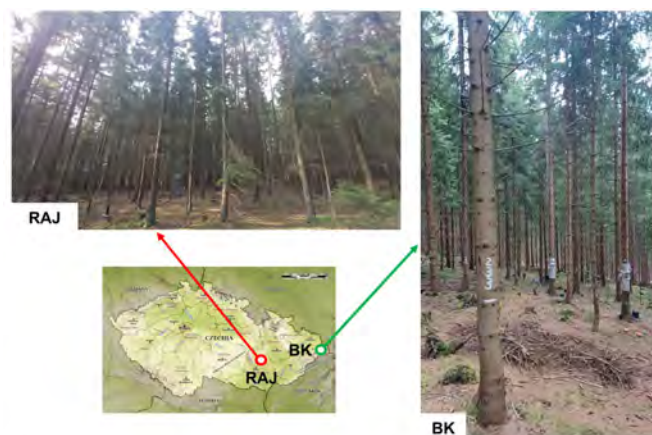
Data Availability Statement: The datasets used or analyzed during the current study are available from the corresponding author upon reasonable request.

Conflicts of Interest: The authors declare that they have no known competing financial interests or financial relationships that could have appeared to influence the work reported in this study.

Abbreviation

FATs	Functional anatomical traits
TRW	Tree-ring width
CWT	Cell wall thickness
LRD	Lumen radial diameter width
EPs	Environmental parameters
CZ	Czech Republic
RAJ	Rájec Nēmčice research plot
BK	Bílý Kříž research plot
EW	Earlywood
LW	Latewood
EWW	Earlywood width
LWW	Latewood width
LWW%	Latewood width percentage
TRD	Tracheid radial diameter width
CLA	Cell lumen area
CWRI	Cell wall reinforcement index
Tair	Air temperature
RH	Relative humidity
PRCP	Precipitation
VPD	Vapour pressure deficit
VPD1.5	threshold value of VPD above 1.5 kPa
SPEI	Standardized Precipitation-Evapotranspiration Index
SPEI-1	one month Standardized Precipitation-Evapotranspiration Index
DE	Drought Event

Appendix A



Site characteristics	Rájec-Němčice (RAJ)	Bílý Kříž (BK)
Location	Drahanská Highlands	Moravian-Silesian Beskydy Mountains
Latitude, N	49°26' N	49°30' N
Longitude, E	16°41' E	18°32' E
Elevation, m a.s.l.	~ 625	~ 875
Soil type	loam-clay Modal Cambisol	Sandy-loam Haplic and Entic Podzol
Soil depth (m)	0.40-0.70	0.60-0.80

Figure A1. Location of the studied research plots in the territory of the Czech Republic (map source: www.bluegreenatlas.com, license: <https://creativecommons.org/licenses/by/4.0/>), including the main site characteristics of the studied research plots [42,44]. View into the inner part of the studied Norway spruce stands. RAJ, Rájec-Němčice; BK, Bílý Kříž.

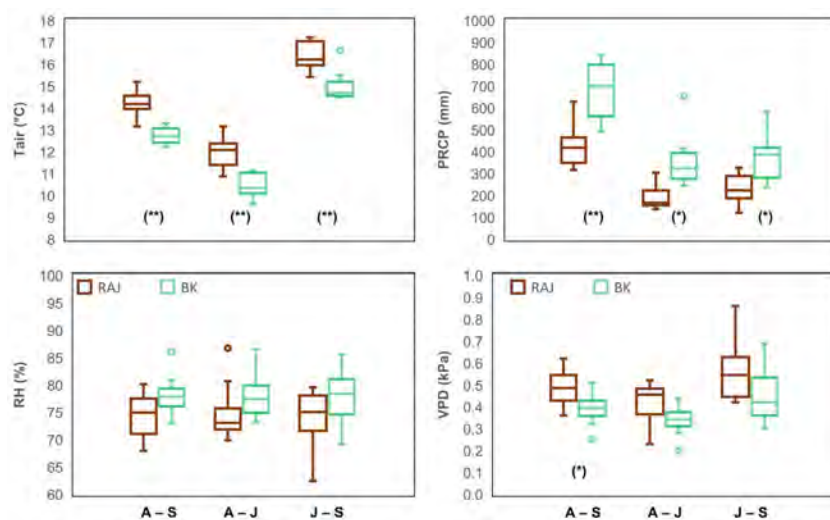


Figure A2. Box plots of the EPs: mean Tair, PRCP, RH, VPD for the growing season (April–September, A–S), and the sub-annual periods of April–June (A–J) and July–September (J–S) in the RAJ and BK plots during the 2010–2017 period. The thick horizontal line in each box plot represents the median value. Each box plot also indicates the upper and lower quartiles, with the vertical lines representing the minimum and maximum values and the outlier points with open circles. Asterisks denote significant differences between the two research plots (* $p < 0.05$, ** $p < 0.01$).

Table A1. Interannual meteorological variability along the Rájec Němčice (RAJ) and Bílý Kříž (BK) plots during the study period 2010–2017. For each time duration (annual, April–September, April–June, and July–September), we calculated the mean air temperature (Tair, °C) and the sum of precipitation (PRCP, mm). We also report the number of days with the extreme threshold value (VPD1.5), with a vapour pressure deficit above 1.5 kPa during the sub-annual periods of April–June and July–September.

RAJ	Annual		April–September		April–June			July–September		
Year	Tair	PRCP	Tair	PRCP	Tair	PRCP	VPD1.5	Tair	PRCP	VPD1.5
2010	6.4	847.1	13.1	628.8	10.9	302.8	0	15.4	326.0	1
2011	8.3	552.7	14.6	399.4	13.0	162.8	0	16.3	236.6	0
2012	8.0	622.1	15.2	316.3	13.2	155.7	3	17.2	160.6	2
2013	7.3	740.9	13.7	497.3	11.3	303.2	0	16.2	194.1	7
2014	8.5	597.1	14.0	435.8	12.2	135.9	3	15.9	299.9	0
2015	8.3	636.4	14.3	359.3	11.4	149.6	0	17.2	209.8	18
2016	7.8	603.1	14.6	315.6	12.1	196.1	0	17.0	119.6	0
2017	7.8	682.6	14.0	453.5	12.1	169.3	2	16.0	284.2	1
BK	Annual		April–September		April–June			July–September		
Year	Tair	PRCP	Tair	PRCP	Tair	PRCP	VPD1.5	Tair	PRCP	VPD1.5
2010	5.6	1518.9	12.2	1235.9	9.9	652.3	0	14.4	583.6	0
2011	6.7	1011.4	13.0	783.6	11.2	387.0	0	14.8	396.6	0
2012	6.4	1064.0	13.3	491.2	11.1	243.4	2	15.5	247.8	3
2013	6.2	1043.2	12.4	570.6	10.3	279.6	0	14.5	291.0	6
2014	7.6	1199.8	12.4	841.2	10.4	415.2	3	14.5	426.0	0
2015	7.4	968.6	13.1	536.4	9.6	299.2	0	16.6	237.2	9
2016	6.6	1268.0	13.1	638.0	11.0	261.2	0	15.1	376.8	0
2017	6.5	1155.4	12.4	759.6	10.1	345.2	0	14.6	414.4	1

References

- Carrer, M.; Motta, R.; Nola, P. Significant Mean and Extreme Climate Sensitivity of Norway Spruce and Silver Fir at Mid-Elevation Mesic Sites in the Alps. *PLoS ONE* **2012**, *7*, e50755. [[CrossRef](#)]
- Amitrano, C.; Arena, C.; Roupheal, Y.; De Pascale, S.; De Micco, V. Vapour Pressure Deficit: The Hidden Driver Behind Plant Morphofunctional Traits in Controlled Environments. *Ann. Appl. Biol.* **2019**, *175*, 313–325. [[CrossRef](#)]
- Fonti, P.; von Arx, G.; García-González, I.; Eilmann, B.; Sass-Klaassen, U.; Gärtner, H.; Eckstein, D. Studying Global Change Through Investigation of the Plastic Responses of Xylem Anatomy in Tree Rings. *New Phytol.* **2010**, *185*, 42–53. [[CrossRef](#)]
- Lachenbruch, B.; McCulloh, K.A. Traits, Properties and Performance: How Woody Plants Combine Hydraulic and Mechanical Functions in a Cell, Tissue or Whole Plant. *New Phytol.* **2014**, *204*, 747–764. [[CrossRef](#)]
- Bussotti, F.; Pollastrini, M.; Holland, V.; Brüggemann, W. Functional Traits and Adaptive Capacity of European Forests to Climate Change. *Environ. Exp. Bot.* **2015**, *111*, 91–113. [[CrossRef](#)]
- Rathgeber, C.B.K.; Fonti, P.; Shishov, V.V.; Rozenberg, P. Wood Formation and Tree Adaptation to Climate. *Ann. For. Sci.* **2019**, *76*, 109. [[CrossRef](#)]
- Song, Y.; Poorter, L.; Horsting, A.; Delzon, S.; Sterck, F. Pit and Tracheid Anatomy Explain Hydraulic Safety but not Hydraulic Efficiency of 28 Conifer Species. *J. Exp. Bot.* **2022**, *73*, 1033–1048. [[CrossRef](#)]
- Matisons, R.; Krišāns, O.; Kārklīna, A.; Adamovičs, A.; Jansons, Ā.; Gärtner, H. Plasticity and Climatic Sensitivity of Wood Anatomy Contribute to Performance of Eastern Baltic Provenances of Scots Pine. *For. Ecol. Manag.* **2019**, *452*, 117568. [[CrossRef](#)]
- Carrer, M.; Castagneri, D.; Prendin, A.L.; Petit, G.; von Arx, G. Retrospective Analysis of Wood Anatomical Traits Reveals a Recent Extension in Tree Cambial Activity in Two High-Elevation Conifers. *Front. Plant Sci.* **2017**, *8*, 737. [[CrossRef](#)]
- Ziaco, E.; Biondi, F.; Rossi, S.; Deslauriers, A. Intra-Annual Wood Anatomical Features of High-Elevation Conifers in the Great Basin, USA. *Dendrochronologia* **2014**, *32*, 303–312. [[CrossRef](#)]
- Gebregorgis, E.G.; Boniecka, J.; Piątkowski, M.; Robertson, I.; Rathgeber, C.B.K. SabaTracheid 1.0: A Novel Program for Quantitative Analysis of Conifer Wood Anatomy—A Demonstration on African Juniper from the Blue Nile Basin. *Front. Plant Sci.* **2021**, *12*, 595258. [[CrossRef](#)]
- von Arx, G.; Crivellaro, A.; Prendin, A.L.; Čufar, K.; Carrer, M. Quantitative Wood Anatomy—Practical Guidelines. *Front. Plant Sci.* **2016**, *1*, 781. [[CrossRef](#)]
- Belokopytova, L.V.; Babushkina, E.A.; Zhirnova, D.F.; Panyushkina, I.P.; Vaganov, E.A. Pine and Larch Tracheids Capture Seasonal Variations of Climatic Signal at Moisture-Limited Sites. *Trees* **2019**, *33*, 227–242. [[CrossRef](#)]

14. Björklund, J.; Seftigen, K.; Schweingruber, F.; Fonti, P.; von Arx, G.; Bryukhanova, M.V.; Cuny, H.E.; Carrer, M.; Castagneri, D.; Frank, D.C. Cell Size and Wall Dimensions Drive Distinct Variability of Earlywood and Latewood Density in Northern Hemisphere Conifers. *New Phytol.* **2017**, *216*, 728–740. [[CrossRef](#)]
15. Bryukhanova, M.; Fonti, P. Xylem Plasticity Allows Rapid Hydraulic Adjustment to Annual Climatic Variability. *Trees* **2013**, *27*, 485–496. [[CrossRef](#)]
16. Castagneri, D.; Fonti, P.; von Arx, G.; Carrer, M. How Does Climate Influence Xylem Morphogenesis Over the Growing Season? Insights from Long-Term Intra-Ring Anatomy in *Picea abies*. *Ann. Bot.* **2017**, *119*, 1011–1020.
17. Fonti, P.; Babushkina, E.A. Tracheid Anatomical Responses to Climate in a Forest-Steppe in Southern Siberia. *Dendrochronologia* **2016**, *39*, 32–41. [[CrossRef](#)]
18. Olano, J.M.; Eugenio, M.; García-Cervigón, A.I.; Folch, M.; Rozas, V. Quantitative Tracheid Anatomy Reveals a Complex Environmental Control of Wood Structure in Continental Mediterranean Climate. *Int. J. Plant Sci.* **2012**, *173*, 137–149. [[CrossRef](#)]
19. Piermattei, A.; von Arx, G.; Avanzi, C.; Fonti, P.; Gärtner, H.; Piotti, A.; Urbinati, C.; Vendramin, G.G.; Büntgen, U.; Crivellaro, A. Functional Relationships of Wood Anatomical Traits in Norway Spruce. *Front. Plant Sci.* **2020**, *11*, 683. [[CrossRef](#)]
20. Choat, B.; Brodribb, T.J.; Brodersen, C.R.; Duursma, R.A.; López, R.; Medlyn, B.E. Triggers of Tree Mortality under Drought. *Nature* **2018**, *558*, 531–539. [[CrossRef](#)]
21. Nilsson, O.; Hjelm, K.; Nilsson, U. Early Growth of Planted Norway Spruce and Scots Pine After Site Preparation in Sweden. *Scand. J. For. Res.* **2019**, *34*, 678–688. [[CrossRef](#)]
22. Lévesque, M.; Saurer, M.; Siegwolf, R.; Eilmann, B.; Brang, P.; Bugmann, H.; Rigling, A. Drought Response of Five Conifer Species Under Contrasting Water Availability Suggests High Vulnerability of Norway Spruce and European Larch. *Glob. Chang. Biol.* **2013**, *19*, 3184–3199. [[CrossRef](#)] [[PubMed](#)]
23. Maringer, J.; Stelzer, A.-S.; Paul, C.; Albrecht, A.T. Ninety-Five Years of Observed Disturbance-Based Tree Mortality Modeled with Climate-Sensitive Accelerated Failure Time Models. *Eur. J. For. Res.* **2021**, *140*, 255–272. [[CrossRef](#)]
24. Hanel, M.; Rakovec, O.; Markonis, Y.; Máca, P.; Samaniego, L.; Kyselý, J.; Kumar, R. Revisiting the Recent European Droughts from a Long-Term Perspective. *Sci. Rep.* **2018**, *8*, 9499. [[CrossRef](#)] [[PubMed](#)]
25. Lindner, M.; Maroschek, M.; Netherer, S.; Kremer, A.; Barbat, A.; Garcia-Gonzalo, J.; Seidl, R.; Delzon, S.; Corona, P.; Kolström, M.; et al. Climate Change Impacts, Adaptive Capacity and Vulnerability of European Forest Ecosystems. *For. Ecol. Manag.* **2010**, *259*, 698–709. [[CrossRef](#)]
26. Kuželková, M.; Jačka, L.; Kovář, M.; Hradilek, V.; Máca, P. Tree Trait-Mediated Differences in Soil Moisture Regimes: A Comparative Study of Beech, Spruce and Larch in a Drought-Prone Area. *Eur. J. For. Res.* **2024**, *143*, 319–332. [[CrossRef](#)]
27. Jevšenak, J.; Tychkov, I.; Gričar, J.; Levanič, T.; Tumajer, J.; Prislán, P.; Arnič, D.; Popkova, M.; Shishov, V.V. Growth-Limiting Factors and Climate Response Variability in Norway Spruce (*Picea abies* L.) Along an Elevation and Precipitation Gradients in Slovenia. *Int. J. Biometeorol.* **2021**, *65*, 311–324. [[CrossRef](#)]
28. Rukh, S.; Poschenrieder, W.; Heym, M.; Pretzsch, H. Drought Resistance of Norway Spruce (*Picea abies* [L.] Karst) and European Beech (*Fagus sylvatica* [L.]) in Mixed vs. Monospecific Stands and on Dry vs. Wet Sites. From Evidence at the Tree Level to Relevance at the Stand Level. *Forests* **2020**, *11*, 639. [[CrossRef](#)]
29. Boden, S.; Kahle, H.-P.; von Wilpert, K.; Spiecker, H. Resilience of Norway Spruce (*Picea abies* (L.) Karst) Growth to Changing Climatic Conditions in Southwest Germany. *For. Ecol. Manag.* **2014**, *315*, 12–21. [[CrossRef](#)]
30. Spathelf, P.; van der Maaten, E.; van der Maaten-Theunissen, M.; Campioli, M.; Dobrowolska, D. Climate Change Impacts in European Forests: The Expert Views of Local Observers. *Ann. For. Sci.* **2014**, *71*, 131–137. [[CrossRef](#)]
31. Tumajer, J.; Altman, J.; Štěpánek, P.; Tremel, V.; Doležal, J.; Cienciala, E. Increasing Moisture Limitation of Norway Spruce in Central Europe Revealed by Forward Modelling of Tree Growth in Tree-Ring Network. *Agric. For. Meteorol.* **2017**, *247*, 56–64. [[CrossRef](#)]
32. Bouche, P.S.; Larter, M.; Domec, J.-C.; Burlett, R.; Gasson, P.; Jansen, S.; Delzon, S. A Broad Survey of Hydraulic and Mechanical Safety in the Xylem of Conifers. *J. Exp. Bot.* **2014**, *65*, 4419–4431. [[CrossRef](#)]
33. Hacke, U.G.; Sperry, J.S. Functional and Ecological Xylem Anatomy. *Perspect. Plant Ecol. Evol. Syst.* **2001**, *4*, 97–115. [[CrossRef](#)]
34. Montwé, D.; Spiecker, H.; Hamann, A. An Experimentally Controlled Extreme Drought in a Norway Spruce Forest Reveals Fast Hydraulic Response and Subsequent Recovery of Growth Rates. *Trees* **2014**, *28*, 891–900. [[CrossRef](#)]
35. Arnič, D.; Gričar, J.; Jevšenak, J.; Božič, G.; von Arx, G.; Prislán, P. Different Wood Anatomical and Growth Responses in European Beech (*Fagus sylvatica* L.) at Three Forest Sites in Slovenia. *Front. Plant Sci.* **2021**, *12*, 669229. [[CrossRef](#)]
36. Lange, J.; Carrer, M.; Pisaric, M.F.J.; Porter, T.J.; Seo, J.-W.; Trouillier, M.; Wilmking, M. Moisture-Driven Shift in the Climate Sensitivity of White Spruce Xylem Anatomical Traits is Coupled to Large-Scale Oscillation Patterns Across Northern Treeline in Northwest North America. *Glob. Chang. Biol.* **2020**, *26*, 1842–1856. [[CrossRef](#)] [[PubMed](#)]
37. Ziaco, E.; Liu, X.; Biondi, F. Dendroanatomy of Xylem Hydraulics in Two Pine Species: Efficiency Prevails on Safety for Basal Area Growth in Drought-Prone Conditions. *Dendrochronologia* **2023**, *81*, 126116. [[CrossRef](#)]
38. Chawla, S.; Nguyen, V.X.; Torres, C.P.G.; Pavelka, M.; Trusina, J.; Marek, M.V. Wind Characteristics Recorded at the Czech Carbon Observation System (CZECOS) Site Rajec. *Eur. J. Environ. Sci.* **2018**, *8*, 117–123. [[CrossRef](#)]
39. Urban, O.; Klem, K.; Ač, A.; Havránková, K.; Holišová, P.; Navrátil, M.; Zitová, M.; Kozlová, K.; Pokorný, R.; Šprtová, M.; et al. Impact of Clear and Cloudy Sky Conditions on the Vertical Distribution of Photosynthetic CO₂ Uptake Within a Spruce Canopy. *Funct. Ecol.* **2012**, *26*, 46–55. [[CrossRef](#)]

40. McGloin, R.; Šigut, L.; Fischer, M.; Foltýnová, L.; Chawla, S.; Trnka, M.; Pavelka, M.; Marek, M.V. Available Energy Partitioning During Drought at two Norway Spruce Forests and a European Beech Forest in Central Europe. *J. Geophys. Res. Atmos.* **2019**, *124*, 3726–3742. [[CrossRef](#)]
41. Sedláč, P.; Aubinet, M.; Heinesch, B.; Janouš, D.; Pavelka, M.; Potužníková, K.; Yernaux, M. Night-Time Airflow in a Forest Canopy near a Mountain Crest. *Agric. For. Meteorol.* **2010**, *150*, 736–744. [[CrossRef](#)]
42. Samec, P.; Voženílek, V.; Vondráková, A.; Macků, J. Diversity of Forest Soils and Bedrock in Soil Regions of the Central-European Highlands (Czech Republic). *Catena* **2018**, *160*, 95–102. [[CrossRef](#)]
43. Kolář, T.; Giagli, K.; Trnka, M.; Bednářová, E.; Vavřík, H.; Rybníček, M. Response of the Leaf Phenology and Tree-Ring Width of European Beech to Climate Variability. *Silva Fenn.* **2016**, *50*, 1520. [[CrossRef](#)]
44. Zapletal, M.; Cudlín, P.; Chroust, P.; Urban, O.; Pokorný, R.; Edwards-Jonášová, M.; Czerný, R.; Janouš, D.; Taufarová, K.; Večeřa, Z.; et al. Ozone Flux over a Norway Spruce Forest and Correlation with Net Ecosystem Production. *Environ. Pollut.* **2011**, *159*, 1024–1034. [[CrossRef](#)] [[PubMed](#)]
45. Gärtner, H.; Nievergelt, D. The Core-Microtome: A new Tool for Surface Preparation on Cores and Time Series Analysis of Varying Cell Parameters. *Dendrochronologia* **2010**, *28*, 85–92. [[CrossRef](#)]
46. Schneider, L.; Gärtner, H. The Advantage of Using a Starch Based Non-Newtonian Fluid to Prepare Micro Sections. *Dendrochronologia* **2013**, *31*, 175–178. [[CrossRef](#)]
47. Pritzkow, C.; Heinrich, I.; Grudd, H.; Helle, G. Relationship Between Wood Anatomy, Tree-Ring Widths and Wood Density of *Pinus sylvestris* L. and Climate at High Latitudes in Northern Sweden. *Dendrochronologia* **2014**, *32*, 295–302. [[CrossRef](#)]
48. Denne, M.P. Definition of Latewood According to Mork (1928). *IAWA J.* **1989**, *10*, 59–62. [[CrossRef](#)]
49. Martin-Benito, D.; Anchukaitis, K.J.; Evans, M.N.; del Río, M.; Beekman, H.; Cañellas, I. Effects of Drought on Xylem Anatomy and Water-Use Efficiency of two Co-Occurring Pine Species. *Forests* **2017**, *8*, 332. [[CrossRef](#)]
50. Pellizzari, E.; Camarero, J.J.; Gazol, A.; Sangüesa-Barreda, G.; Carrer, M. Wood Anatomy and Carbon-Isotope Discrimination Support Long-Term Hydraulic Deterioration as a Major Cause of Drought-Induced Dieback. *Glob. Chang. Biol.* **2016**, *22*, 2125–2137. [[CrossRef](#)]
51. Fajstavr, M.; Giagli, K.; Vavřík, H.; Gryc, V.; Horáček, P.; Urban, J. The Cambial Response of Scots Pine Trees to Girdling and Water Stress. *IAWA J.* **2020**, *41*, 159–185. [[CrossRef](#)]
52. Fillion, L.; Cournoyer, L. Variation in Wood Structure of Eastern Larch Defoliated by the Larch Sawfly in Subarctic Quebec, Canada. *Can. J. For. Res.* **1995**, *25*, 1263–1268. [[CrossRef](#)]
53. Campelo, F.; Nabais, C.; Carvalho, A.; Vieira, J. TracheideR- An R Package to Standardize Tracheidograms. *Dendrochronologia* **2016**, *37*, 64–68. [[CrossRef](#)]
54. Broz, A.; Retallack, G.J.; Maxwell, T.M.; Silva, L.C.R. A Record of Vapour Pressure Deficit Preserved in Wood and Soil Across Biomes. *Sci. Rep.* **2021**, *11*, 662. [[CrossRef](#)] [[PubMed](#)]
55. Hoylman, Z.H.; Jencso, K.G.I.; Hu, J.; Holden, Z.A.; Martin, J.T.; Gardner, W.P. The Climatic Water Balance and Topography Control Spatial Patterns of Atmospheric Demand, Soil Moisture and Shallow Subsurface Flow. *Water Resour. Res.* **2019**, *55*, 2370–2389. [[CrossRef](#)]
56. de Cárcer, P.S.; Vitasse, Y.; Peñuelas, J.; Jasse, V.E.J.; Buttler, A.; Signarbieux, C. Vapor-Pressure Deficit and Extreme Climatic Variables Limit Tree Growth. *Glob. Chang. Biol.* **2018**, *24*, 1108–1122. [[CrossRef](#)] [[PubMed](#)]
57. McKee, T.B.; Doesken, N.J.; Kleist, J. The Relationship of Drought Frequency and Duration to Time Scales. In Proceedings of the 8th Conference on Applied Climatology, Anaheim, CA, USA, 17–22 January 1993; pp. 179–183.
58. Manning, C.; Widmann, M.; Bevacqua, E.; Van Loon, A.F.; Maraun, D.; Vrac, M. Soil Moisture Drought in Europe: A Compound Event of Precipitation and Potential Evapotranspiration on Multiple Time Scales. *J. Hydrometeorol.* **2018**, *19*, 1255–1271. [[CrossRef](#)]
59. Quiring, S.M. Developing Objective Operational Definitions for Monitoring Drought. *J. Appl. Meteorol. Climatol.* **2009**, *48*, 1217–1229. [[CrossRef](#)]
60. Vicente-Serrano, S.M.; Peña-Angulo, D.; Murphy, C.; López-Moreno, J.I.; Tomas-Burguera, M.; Domínguez-Castro, F.; Tian, F.; Eklundh, L.; Cai, Z.; Alvarez-Farizo, B.; et al. The Complex Multisectoral Impacts of Drought: Evidence from a Mountainous Basin in the Central Spanish Pyrenees. *Sci. Total Environ.* **2021**, *769*, 144702. [[CrossRef](#)]
61. Parente, J.; Amraoui, M.; Menezes, I.; Pereira, M.G. Drought in Portugal: Current Regime, Comparison of Indices and Impacts on Extreme Wildfires. *Sci. Total Environ.* **2019**, *685*, 150–173. [[CrossRef](#)]
62. Spinoni, J.; Naumann, G.; Vogt, J.; Barbosa, P. European Drought Climatologies and Trends Based on a Multi-Indicator Approach. *Glob. Planet. Chang.* **2015**, *127*, 50–57. [[CrossRef](#)]
63. Vicente-Serrano, S.M.; Beguería, S.; López-Moreno, J.I. A Multiscalar Drought Index Sensitive to Global Warming: The Standardized Precipitation Evapotranspiration Index. *J. Clim.* **2010**, *23*, 1696–1718. [[CrossRef](#)]
64. Newson, R. Parameters Behind ‘Non-Parametric’ Statistics: Kendall’s tau, Somers’ D and median differences. *Stata J.* **2002**, *2*, 45–64. [[CrossRef](#)]
65. Zahradníček, P.; Brázdil, R.; Řehoř, J.; Lhotka, O.; Dobrovolný, P.; Štěpánek, P.; Trnka, M. Temperature Extremes and Circulation Types in the Czech Republic, 1961–2020. *Int. J. Climatol.* **2022**, *42*, 4808–4829. [[CrossRef](#)]
66. Luostarinen, K.; Pikkariainen, L.; Ikonen, V.-P.; Gerendiain, A.Z.; Pulkkinen, P.; Peltola, H. Relationships of Wood Anatomy with Growth and Wood Density in Three Norway Spruce Clones of Finnish Origin. *Can. J. For. Res.* **2017**, *47*, 1184–1192. [[CrossRef](#)]

67. Gričar, J.; Prislán, P.; de Luis, M.; Gryc, V.; Hacurová, J.; Vavrčík, H.; Čufar, K. Plasticity in Variation of Xylem and Phloem Cell Characteristics of Norway Spruce Under Different Local Conditions. *Front. Plant Sci.* **2015**, *6*, 730. [[CrossRef](#)] [[PubMed](#)]
68. Rathgeber, C.B.K. Conifer Tree-Ring Density Inter-Annual Variability—Anatomical, Physiological and Environmental Determinants. *New Phytol.* **2017**, *216*, 621–625. [[CrossRef](#)] [[PubMed](#)]
69. Pittermann, J.; Sperry, J.S.; Wheeler, J.K.; Hacke, U.G.; Sikkema, E.H. Mechanical Reinforcement of Tracheids Compromises the Hydraulic Efficiency of Conifer Xylem. *Plant Cell Environ.* **2006**, *29*, 1618–1628. [[CrossRef](#)] [[PubMed](#)]
70. Rosner, S.; Gierlinger, N.; Klepsch, M.; Karlsson, B.; Evans, R.; Lundqvist, S.-O.; Světlík, J.; Børja, I.; Dalsgaard, L.; Andreassen, K.; et al. Hydraulic and Mechanical Dysfunction of Norway Spruce Sapwood due to Extreme Summer Drought in Scandinavia. *For. Ecol. Manag.* **2018**, *409*, 527–540. [[CrossRef](#)]
71. Liang, C.; Fillion, L.; Cournoyer, L. Wood Structure of Biotically and Climatically Induced Light Rings in Eastern Larch (*Larix laricina*). *Can. J. For. Res.* **1997**, *27*, 1538–1547. [[CrossRef](#)]
72. Lhotka, O.; Trnka, M.; Kyselý, J.; Markonis, Y.; Balek, J.; Možný, M. Atmospheric Circulation as a Factor Contributing to Increasing Drought Severity in Central Europe. *J. Geophys. Res. Atmos.* **2020**, *125*, e2019JD032269. [[CrossRef](#)]
73. Buras, A.; Schunk, C.; Zeiträg, C.; Herrmann, C.; Kaiser, L.; Lemme, H.; Straub, C.; Taeger, S.; Gößwein, S.; Klemmt, H.-J.; et al. Are Scots Pine Forest Edges Particularly Prone to Drought-Induced Mortality? *Environ. Res. Lett.* **2018**, *13*, 025001. [[CrossRef](#)]
74. Burri, S.; Haeler, E.; Eugster, W.; Haeni, M.; Etzold, S.; Walthert, L.; Braun, S.; Zweifel, R. How did Swiss Forest Trees Respond to the Hot Summer 2015? *Die Erde* **2019**, *150*, 214–229.
75. Trnka, M.; Brázdil, R.; Balek, J.; Semerádová, D.; Hlavinka, P.; Možný, M.; Štěpánek, P.; Dobrovolný, P.; Zahradníček, P.; Dubrovský, M.; et al. Drivers of Soil Drying in the Czech Republic Between 1961 and 2012. *Int. J. Climatol.* **2015**, *35*, 2664–2675. [[CrossRef](#)]
76. Mensah, C.; Šigut, L.; Fischer, M.; Foltýnová, L.; Jocher, G.; Urban, O.; Wemegah, C.S.; Nyantakyi, E.K.; Chawla, S.; Pavelka, M.; et al. Environmental Effects on Normalized Gross Primary Productivity in Beech and Norway Spruce Forests. *Atmosphere* **2021**, *12*, 1128. [[CrossRef](#)]
77. Cui, Z.; Wang, Y.; Zhang, G.J.; Yang, M.; Liu, J.; Wei, L. Effects of Improved Simulation of Precipitation on Evapotranspiration and Its Partitioning Over Land. *Geophys. Res. Lett.* **2022**, *49*, e2021GL097353. [[CrossRef](#)]
78. Liu, Y.; Jiang, Q.; Wang, Q.; Jin, Y.; Yue, Q.; Yu, J.; Zheng, Y.; Jiang, W.; Yao, X. The Divergence Between Potential and Actual Evapotranspiration: An Insight from Climate, Water and Vegetation Change. *Sci. Total Environ.* **2022**, *807*, 150648. [[CrossRef](#)]
79. Daněk, P.; Šamonil, P.; Vrška, T. Four Decades of the Coexistence of Beech and Spruce in a Central European Old-Growth Forest. Which Succeeds on what Soils and Why? *Plant Soil* **2019**, *437*, 257–272. [[CrossRef](#)]

Disclaimer/Publisher’s Note: The statements, opinions and data contained in all publications are solely those of the individual author(s) and contributor(s) and not of MDPI and/or the editor(s). MDPI and/or the editor(s) disclaim responsibility for any injury to people or property resulting from any ideas, methods, instructions or products referred to in the content.